arXiv:2101.09048v3 [cs.LG] 15 Jun 2021

Selfish Sparse RNN Training

Shiwei Liu [1] **Decebal Constantin Mocanu** [1 2] **Yulong Pei** [1] **Mykola Pechenizkiy** [1]

Abstract

Sparse neural networks have been widely applied to reduce the computational demands of training and deploying over-parameterized deep neural networks. For inference acceleration, methods that discover a sparse network from a pre-trained dense network (dense-to-sparse training) work effectively. Recently, dynamic sparse training (DST) has been proposed to train sparse neural networks without pre-training a dense model (sparse-to-sparse training), so that the training process can also be accelerated. However, previous sparse-to-sparse methods mainly focus on Multilayer Perceptron Networks (MLPs) and Convolutional Neural Networks (CNNs), failing to match the performance of dense-to-sparse methods in the Recurrent Neural Networks (RNNs) setting. In this paper, we propose an approach to train intrinsically sparse RNNs with a fixed parameter count in one single run, without compromising performance. During training, we allow RNN layers to have a non-uniform redistribution across cell gates for better regularization. Further, we propose SNT-ASGD, a novel variant of the averaged stochastic gradient optimizer, which significantly improves the performance of all sparse training methods for RNNs. Using these strategies, we achieve state-of-the-art sparse training results, better than the dense-to-sparse methods, with various types of RNNs on Penn TreeBank and Wikitext-2 datasets. Our codes are available at https://github.com/Shiweiliuiiiiiii/Selfish-RNN.

[1]Department of Computer Science, Eindhoven University of Technology, the Netherlands
[2]Faculty of Electrical Engineering, Mathematics, and Computer Science at University of Twente, the Netherlands
. Correspondence to: Shiwei Liu <s.liu3@tue.nl>.

Proceedings of the 38^{th} International Conference on Machine Learning, PMLR 139, 2021. Copyright 2021 by the author(s).

1. Introduction

Recurrent neural networks (RNNs) (Elman, 1990), with a variant of long short-term memory (LSTM) (Hochreiter & Schmidhuber, 1997), have been highly successful in various fields, including language modeling (Mikolov et al., 2010), machine translation (Kalchbrenner & Blunsom, 2013), question answering (Hirschman et al., 1999; Wang & Jiang, 2017), etc. As a standard task to evaluate models' ability to capture long-range context, language modeling has witnessed great progress in RNNs. Mikolov et al. (2010) demonstrated that RNNs perform much better than backoff models for language modeling. After that, various novel RNN architectures such as Recurrent Highway Networks (RHNs) (Zilly et al., 2017), Pointer Sentinel Mixture Models (Merity et al., 2017), Neural Cache Model (Grave et al., 2017), Mixture of Softmaxes (AWD-LSTM-MoS) (Yang et al., 2018), Ordered Neurons LSTM (ON-LSTM) (Shen et al., 2019), and effective regularization like Variational Dropout (Gal & Ghahramani, 2016), Weight Tying (Inan et al., 2017), DropConnect (Merity et al., 2018) have been proposed to improve the performance of RNNs on language modeling.

At the same time, as the performance of deep neural networks (DNNs) improves, the resources required to train and deploy these deep models are becoming prohibitively large. To tackle this problem, various dense-to-sparse methods have been developed, including but not limited to pruning (LeCun et al., 1990; Han et al., 2015; Molchanov et al., 2016), variational dropout (Kingma et al., 2015; Molchanov et al., 2017), distillation (Hinton et al., 2015), L_1 regularization (Wen et al., 2018), and low-rank decomposition (Jaderberg et al., 2014). Given a pre-trained model, these methods work effectively to accelerate the inference process.

Recently, some dynamic sparse training (DST) approaches (Mocanu et al., 2018; Mostafa & Wang, 2019; Dettmers & Zettlemoyer, 2019; Evci et al., 2020) have been proposed to bring efficiency to the training phase as well. However, previous approaches are mainly for CNNs and MLPs. The long-term dependencies and repetitive usage of recurrent cells make RNNs more difficult to be sparsified (Kalchbrenner et al., 2018; Evci et al., 2020). More importantly, the state-of-the-art performance achieved by RNNs on language modeling is mainly associated with the optimizer, averaged

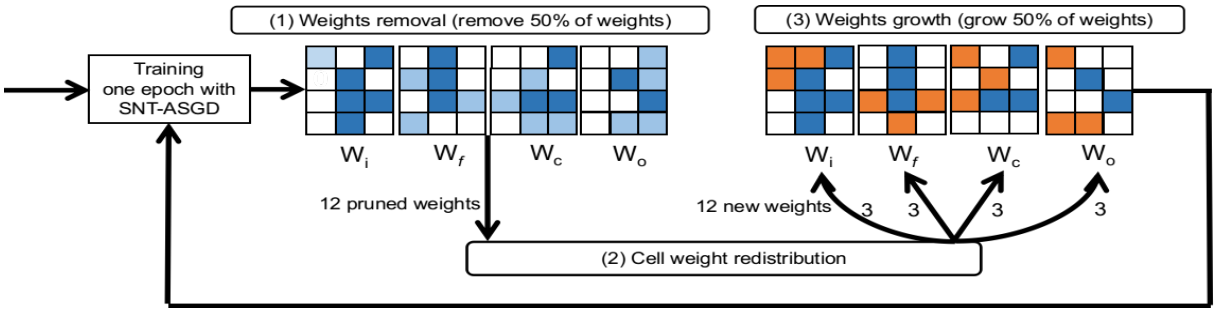


Figure 1. Schematic diagram of the Selfish-RNN. W_i, W_f, W_c, W_o refer to LSTM cell gates. Colored squares and white squares refer to nonzero weights and zero weights, respectively. Light blue squares are weights to be removed and orange squares are weights to be grown.

stochastic gradient descent (ASGD) (Polyak & Juditsky, 1992), which is not compatible with the existing DST approaches. The abovementioned problems heavily limit the performance of the off-the-shelf sparse training methods in the RNN field. For instance, while "The Rigged Lottery" (RigL) achieves state-of-the-art sparse training results with various CNNs, it fails to match the performance of the iterative pruning method (Gale et al., 2019) in the RNN setting (Evci et al., 2020).

In this paper, we propose an algorithm to train initially sparse RNNs with a fixed number of parameters throughout training. We abbreviate our sparse RNN training method as Selfish-RNN because our method encourages cell gates to obtain their parameters selfishly. The main contributions of this work are four-fold:

- We propose an algorithm to train sparse RNNs from scratch with a fixed number of parameters. Our method has two novelty components: (1) we propose SNT-ASGD, a sparse variant of the non-monotonically triggered averaged stochastic gradient descent optimizer (NT-ASGD), which improves the performance of all sparse training methods for RNNs; (2) we allow RNN layers to have a non-uniform redistribution across cell gates during training for a better regularization.

- We demonstrate state-of-the-art sparse training performance, better than the dense-to-sparse methods, with various RNN models, including stacked LSTMs (Zaremba et al., 2014), RHNs, ON-LSTM on Penn TreeBank (PTB) dataset (Marcus et al., 1993) and AWD-LSTM-MoS on WikiText-2 dataset (Melis et al., 2018).

- We present an approach to measure the topological distance between different sparse connectivities from the perspective of graph theory. Recent works (Garipov et al., 2018; Draxler et al., 2018; Fort & Jastrzebski, 2019) on understanding dense loss landscapes find that many independent optima are located in different low-loss tunnels. We complement these works by showing that there exist many low-loss sparse networks which are very different in the topological space.

- Our analysis shows two surprising phenomena in the setting of RNNs contrary to CNNs (1) random-based weight growth performs better than gradient-based weight growth, and (2) uniform sparse distribution performs better than *Erdős-Rényi* (ER) sparse distribution. These results highlight the need to choose different sparse training methods for different architectures.

2. Related Work

Dense-to-Sparse. There are a large number of works operating on a dense network to yield a sparse network. We divide them into three categories based on the training cost in terms of memory and computation.
(1) *Iterative Pruning and Retraining.* To the best of our knowledge, pruning was first proposed by Janowsky (1989) and Mozer & Smolensky (1989) whose goal is to yield a sparse network from a pre-trained network for sparse inference. Han et al. (2015) brought it back to people's attention based on the idea of iterative pruning and retraining with modern architectures. Gradual Magnitude Pruning (GMP) (Zhu & Gupta, 2017; Gale et al., 2019) was further proposed to obtain the target sparse model in one running. Recently, Frankle & Carbin (2019) proposed the Lottery Ticket Hypothesis showing that the sub-networks ("winning tickets") obtained via iterative magnitude pruning combined with their "lucky" initialization can outperform the dense networks. Zhou et al. (2019) found that the sign of the initial weights is the key factor that makes the "winning tickets" work. Our work shows that there exists a much more efficient and robust way to find those "winning tickets" without any pre-training steps and any specific initialization. Overall, iterative pruning and retraining requires at least the same training cost as training a dense model, sometimes even

Table 1. Comparison of different sparsity-inducing approaches in RNNs. ER and ERK refer to the *Erdős-Rényi* distribution and the *Erdős-Rényi-Kernel* distribution, respectively. *Backward Sparse* means a clean sparse backward pass and no need to compute or store any information of the non-existing weights. *Sparse Opt* indicates whether a specific optimizer is proposed for sparse RNN training.

Method	Initialization	Removal	Growth	Weight Redistribution	Backward Sparse	Sparse Opt
Iterative Pruning	dense	$min(\|\theta\|)$	none	no	no	no
ISS	dense	Lasso	none	no	no	no
SET	ER	$min(\|\theta\|)$	random	no	yes	no
DSR	uniform	$min(\|\theta\|)$	random	across all layers	yes	no
SNFS	uniform	$min(\|\theta\|)$	momentum	across all layers	no	no
RigL	ERK	$min(\|\theta\|)$	gradient	no	no	no
Selfish-RNN	uniform	$min(\|\theta\|)$	random	across RNN cell gates	yes	yes

more, as a pre-trained dense model is involved. We compare our method with the state-of-the-art pruning method proposed by Zhu & Gupta (2017) in Appendix I. With fewer training costs, our method is able to discover sparse networks with lower test perplexity.

(2) *Learning Sparsity During Training.* Some works attempt to learn the sparse networks during training. Louizos et al. (2017) and Wen et al. (2018) were examples that gradually enforce the network weights to zero via L_0 and L_1 regularization, respectively. Dai et al. (2018) proposed the idea of using singular value decomposition (SVD) to accelerate the training process for LSTMs. Recent works (Liu et al., 2020a; Srivastava et al., 2015; Xiao et al., 2019; Kusupati et al., 2020) induce sparsity by jointly learning masks and model weights during training. These methods start with a fully dense network, and hence are not memory efficient.

(3) *Pruning at Initialization.* Some works aim to find sparse neural networks by pruning once prior to the main training phase based on some salience criteria, including connection sensitivity (Lee et al., 2019; 2020), synaptic flow (Tanaka et al., 2020), gradient signal preservation (Wang et al., 2020), and iterative pruning (de Jorge et al., 2020). These techniques can find sparse networks before the standard training, but at least one iteration of dense training is involved to identify these trainable sparse networks. Additionally, pruning at initialization generally cannot match the performance of dynamic sparse training, especially at extreme sparsity levels (Wang et al., 2020).

Sparse-to-Sparse. Recently, many works have emerged to train intrinsically sparse neural networks from scratch to obtain efficiency both for training and inference.

(1) *Static Sparse Training.* Mocanu et al. (2016) developed intrinsically sparse networks by exploring the scale-free and small-world topological properties in Restricted Boltzmann Machines. Later, some works focus on designing sparse CNNs based on Expander graphs and show comparable performance against the corresponding dense models (Prabhu et al., 2018; Kepner & Robinett, 2019).

(2) *Dynamic Sparse Training.* Mocanu et al. (2018) proposed Sparse Evolutionary Training (SET) allowing sparse training MLPs to match the performance of dense MLPs by dynamically changing the sparse connectivity based on a simple remove-and-regrow strategy. Shortly after, DeepR was introduced by Bellec et al. (2018) to train sparse networks by sampling the sparse connectivity from the posterior distribution. Mostafa & Wang (2019) introduced Dynamic Sparse Reparameterization (DSR) to train sparse neural networks while dynamically adjusting the sparse distribution during training. Sparse Networks from Scratch (SNFS) (Dettmers & Zettlemoyer, 2019) improved the sparse training performance by introducing the idea of growing free weights according to their momentum. While effective, it requires extra computation and memory to update the dense momentum tensor for every iteration. RigL (Evci et al., 2020) went one step further by activating new weights with the highest magnitude gradient. It amortizes the significant amount of overhead by updating the sparse connectivity infrequently. In addition, some recent works (Jayakumar et al., 2020; Raihan & Aamodt, 2020) attempt to explore more sparse space during training to improve the sparse training performance. Due to the inherent limitations of deep learning software and hardware libraries, all of those works simulate sparsity using a binary mask over weights. More recently, Liu et al. (2020b) proved the practical values of DST by developing for the first time an independent software framework to train truly sparse MLPs with over one million neurons on a typical laptop. However, all these works mainly focus on CNNs and MLPs, and they are not designed to match state-of-the-art performance for RNNs.

We summarize the properties of all approaches compared in this paper in Table 1. Additionally, we provide a high-level overview of the difference between Selfish-RNN and iterative pruning and re-training in Figure 2. FLOPs required by Selfish-RNN is much smaller than iterative pruning and re-training, as it starts with a sparse network and without any retraining phases. See Appendix H for more differences.

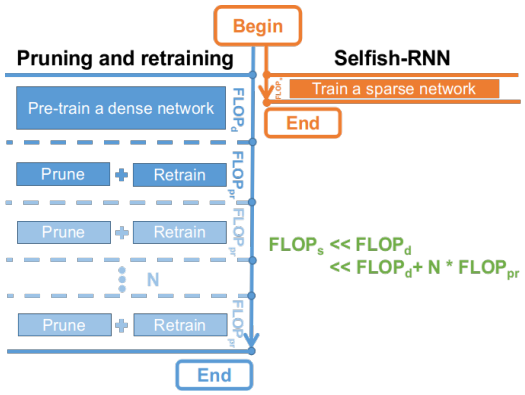


Figure 2. A high-level overview of the difference between Selfish-RNN and iterative pruning and re-training techniques. Blocks with light blue color represent optional pruning and retraining steps chosen depending on specific approaches.

Algorithm 1 Selfish-RNN

Input: Model weight θ, number of layer L, sparsity S, pruning rate p, training epoch n
for $i = 1$ **to** L **do**
  Initialize the network with Eq. (1)
end for
for $epoch = 1$ **to** n **do**
  Training: $\theta_s \leftarrow$ SNT-ASGD(θ_s)
  for $i = 1$ **to** L **do**
    if RNN layer **then**
      Cell Gate redistribution with Eq. (4)
    else
      Weight removal with Eq. (2)
      Weight growth with Eq. (3)
    end if
  end for
  $p \leftarrow$DecayRemovingRate(p)
end for

3. Sparse RNN Training

Our sparse RNN training method is illustrated in Figure 1 with LSTM as a specific case. Note that our method can be easily applied to any other RNN variants. The only difference is the number of cell gates. Before training, we randomly initialize each layer at the same sparsity (the fraction of zero-valued weights), so that the training costs are proportional to the dense model at the beginning. To explore more sparse structures, while to maintain a fixed sparsity level, we need to optimize the sparse connectivity together with the corresponding weights (a combinatorial optimization problem). We use dynamic sparse connectivity and SNT-ASGD together to handle this combinatorial optimization problem. The pseudocode of the full training procedure of our algorithm is shown in Algorithm 1.

3.1. Dynamic Sparse Connectivity

We consider uniform sparse initialization, magnitude weight removal, random weight growth, and cell gate redistribution together as main components of our dynamic sparse training method, which can ensure a fixed number of parameters and a clean sparse backward pass, as discussed next.

Notation. Given a dataset of N samples $\mathbf{D} = \{(x_i, y_i)\}_{i=1}^{N}$ and a network $f(x;\theta)$ parameterized by θ. We train the network to minimize the loss function $\sum_{i=1}^{N} L(f(x_i;\theta), y_i)$. The basic mechanism of sparse training is to train with a fraction of parameters θ_s, while preserving the performance as much as possible. Hence, a sparse neural network can be denoted as $f_s(x;\theta_s)$ with a sparsity level $S = 1 - \frac{\|\theta_s\|_0}{\|\theta\|_0}$, where $\|\cdot\|_0$ is the ℓ_0-norm.

Uniform Sparse Initialization. First, the network is randomly initialized with a uniform sparse distribution in which the sparsity level of each layer is the same S. More precisely, the network is initialized by:

$$\theta_s = \theta \odot M \tag{1}$$

where θ is a dense weight tensor initialized in a standard way; M is a binary tensor, in which nonzero elements are sampled uniformly based on the sparsity S; $\odot$ refers to the Hadamard product.

Magnitude Weight Removal. For non-RNN layers, we use magnitude weight removal followed by random weight growth to update the sparse connectivity. We remove a fraction p of weights with the smallest magnitude after each training epoch. This step is performed by changing the binary tensor M, as follows:

$$M = M - P \tag{2}$$

where P is a binary tensor with the same shape as M, in which the nonzero elements have the same indices with the top-p smallest-magnitude nonzero weights in θ_s, with $||P||_0 = p||M||_0$.

Random Weight Growth. To keep a fixed parameter count, we randomly grow the same number of weights immediately after weight removal, by:

$$M = M + R \tag{3}$$

where R is a binary tensor where the nonzero elements are randomly located at the position of zero elements of M. We choose random growth to get rid of using any information of the non-existing weights, so that both feedforward and backpropagation are completely sparse. It is more desirable to have such pure sparse structures as it enables the possibility of conceiving in the future specialized hardware accelerators for sparse neural networks. Besides, our analysis of

growth methods in Section 5.2 shows that random growth can explore more sparse structural degrees of freedom than gradient growth, which might be crucial to sparse training.

Cell Gate Redistribution. Our dynamic sparse connectivity differs from previous methods mainly in cell gate redistribution. For non-RNN layers, we use magnitude weight removal followed by random weight growth to update the sparse connectivity. For RNN layers, we use cell gate redistribution to update their sparse connectivities. The naive approach is to sparsify all cell gates independently at the same sparsity, as used in Liu et al. (2019) which is a straightforward SET extension to RNNs. Essentially, it is more desirable to redistribute new weights to cell gates dependently, as all gates collaborate together to regulate information. Intuitively, we redistribute new weights in a way that cell gates containing more large-magnitude weights should have more weights. Large-magnitude weights indicate that their loss gradients are large and few oscillations occur. Therefore, gates with more large-magnitude weights should be reallocated with more parameters to accelerate training. Concretely, for each RNN layer l, we remove weights dependently given by an ascending sort:

$$Sort_p(|\theta_1^l|, |\theta_2^l|, .., |\theta_t^l|) \tag{4}$$

where $\{\theta_1^l, \theta_2^l, ..., \theta_t^l\}$ are all gate tensors within RNN cell, and $Sort_p$ returns p indices of the smallest-magnitude weights. After weight removal, new weights are uniformly grown to each gate, so that gates with more large-magnitude weights will gradually obtain more weights. We further demonstrate the final sparsity breakdown of cell gates learned by our method in Appendix M and observe that the forget gates are consistently sparser than other gates for all models.

Similar with SNFS, We also decay the pruning rate p to zero with a cosine annealing. We further use Eq. (1) to enforce the sparse structure before the forward pass and after the backward pass, so that zero weights will not contribute to the loss. And all newly activated weights are initialized to zero.

3.2. Sparse Non-monotonically Triggered ASGD

Non-monotonically Triggered ASGD (NT-ASGD) has shown its ability to achieve remarkable performance with various RNNs (Merity et al., 2018; Yang et al., 2018; Shen et al., 2019). However, it becomes less appealing for sparse RNNs training. Unlike dense networks in which every parameter in the model is updated at each iteration, the non-active weights remain zero for sparse training. Once these non-active weights are activated, the original averaging operation of standard NT-ASGD will immediately bring them close to zero. Thereby, after the averaging operation is triggered, the number of valid weights will decrease sharply. To alleviate this problem, we describe SNT-ASGD as following:

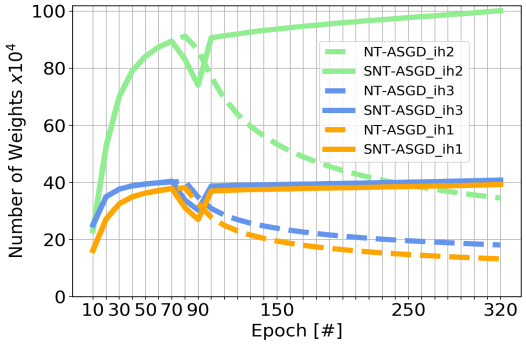


Figure 3. The number of weights whose magnitude is larger than 0.1 during training for ON-LSTM. The solid lines represent SNT-ASGD and dashed lines represent standard NT-ASGD. *ih1*, *ih2*, and *ih3* refer to input weights in the first, second and third LSTM layer.

$$\tilde{w}_i = \begin{cases} 0 & if\ m_i = 0, \forall i, \\ \frac{\sum_{t=T_i}^{K} w_{i,t}}{(K - T_i + 1)} & if\ m_i = 1, \forall i. \end{cases} \tag{5}$$

where $\tilde{w}_i$ is the value returned by SNT-ASGD for weight w_i; $w_{i,t}$ represents the actual value of weight w_i at the t^{th} iteration; $m_i = 1$ if the weight w_i exists and $m_i = 0$ if not; T_i is the iteration in which the weight w_i grows most recently; and K is the total number of iterations. We demonstrate the effectiveness of SNT-ASGD in Figure 3. At the beginning when trained with SGD, the number of weights with high magnitude increases fast. However, the trend of NT-ASGD starts to descend significantly once the averaging is triggered at epoch 80, whereas the trend of SNT-ASGD continues to rise after a small drop caused by the averaging operation.

Besides, the constant learning rate of SNT-ASGD helps to prevent the negative effect of learning rate decay on dynamic sparse training. Since most dynamic sparse training methods initialize the newly activated weights as zero, the magnitude of new weights can barely catch up with the unpruned weights once the learning rate is decayed to small values. To better understand how proposed components, cell gate redistribution and SNT-ASGD, improve the sparse RNN training performance, we further conduct an ablation study in Appendix B. It is clear to see that both of them lead to significant performance improvement.

4. Experimental Results

We evaluate Selfish-RNN with various models including stacked LSTMs, RHNs, ON-LSTM on the Penn TreeBank dataset and AWD-LSTM-MoS on the WikiText-2 dataset. The performance of Selfish-RNN is compared with 6 state-of-the-art sparse inducing techniques, including 2 dense-to-sparse methods, ISS and GMP; 4 sparse-to-sparse methods,

Table 2. Single model perplexity on validation and test sets for the Penn Treebank language modeling task with stacked LSTMs and RHNs. '*' indicates the reported results from the original papers: "Dense" is obtained from Zaremba et al. (2014) and ISS is obtained from Wen et al. (2018). "Static-ER" and "Static-Uniform" are the static sparse network trained from scratch with ER distribution and uniform distribution, respectively. "Small Dense" refers to the small dense network with the same number of parameters as Selfish-RNN.

	Stacked LSTMs			RHNs		
Models	#Parameters	Validation	Test	#Parameters	Validation	Test
Dense*	66.0M	82.57	78.57	23.5M	67.90	65.40
Dense (NT-ASGD)	66.0M	74.51	72.40	23.5M	63.44	61.84
	Sparsity=0.67			Sparsity=0.53		
Small Dense (NT-ASGD)	21.8M	88.67	86.33	11.1M	70.10	68.40
Static-ER (SNT-ASGD)	21.8M	81.02	79.30	11.1M	75.74	73.21
Static-Uniform (SNT-ASGD)	21.8M	80.37	78.61	11.1M	74.11	71.83
ISS*	21.8M	82.59	78.65	11.1M	68.10	65.40
DSR (Adam)	21.8M	89.95	88.16	11.1M	65.38	63.19
GMP (Adam)	21.8M	89.47	87.97	11.1M	63.21	61.55
SNFS (Adam)	21.8M	88.31	86.28	11.1M	74.02	70.99
RigL (Adam)	21.8M	88.39	85.61	11.1M	67.43	64.41
SET (Adam)	21.8M	87.30	85.49	11.1M	63.66	61.08
Selfish-RNN (Adam)	21.8M	85.70	82.85	11.1M	63.28	60.75
RigL (SNT-ASGD)	21.8M	78.31	75.90	11.1M	64.82	62.47
GMP (SNT-ASGD)	21.8M	76.78	74.84	11.1M	65.63	63.96
Selfish-RNN (SNT-ASGD)	21.8M	**73.76**	**71.65**	11.1M	**62.10**	**60.35**
	Sparsity=0.62			Sparsity=0.68		
ISS*	25.2M	80.24	76.03	7.6M	70.30	67.70
RigL (SNT-ASGD)	25.2M	77.16	74.76	7.6M	69.32	66.64
GMP (SNT-ASGD)	25.2M	74.86	73.03	7.6M	66.61	64.98
Selfish-RNN (SNT-ASGD)	25.2M	**73.50**	**71.42**	7.6M	**66.35**	**64.03**

SET, DSR, SNFS, and RigL. Intrinsic Sparse Structures (ISS) (Wen et al., 2018) is a method that uses Lasso regularization to explore sparsity inside RNNs. GMP is the state-of-the-art unstructured pruning method in DNNs. For fair comparison, we use the exact same hyperparameters and regularization introduced in ON-LSTM (Shen et al., 2019) and AWD-LSTM-MoS (Yang et al., 2018). We then extend these similar settings to stacked LSTMs and RHNs. We choose Adam (Kingma & Ba, 2014) and SNT-ASGD as the optimizers of different DST methods. Due to the space limitation, we put the results of sparse ON-LSTM on PTB and sparse AWD-LSTM-MoS on Wikitext-2 in Appendix D and Appendix E, respectively. See Appendix A for hyperparameters.

4.1. Stacked LSTMs

As introduced by Zaremba et al. (2014), stacked LSTMs (large) is a two-layer LSTM model with 1500 hidden units for each LSTM layer. We choose the same sparsity as ISS, 67% and 62%. Results are shown in the left side of Table 2 (see Appendix L for the version with estimated FLOPs). We provide a new dense baseline trained with the standard NT-ASGD, achieving 6 lower test perplexity than the widely-used baseline. When optimized by Adam, while Selfish-RNN achieves the lowest perplexity, all sparse training techniques fail to match the performance of ISS and dense models. On the other hand, training sparse RNNs with SNT-ASGD substantially improves the performance of all sparse methods, and Selfish-RNN achieves the best one, even better than the new dense baseline. Note that even starting from a sparse network (sparse-to-sparse), our method can discover a better solution than the state-of-the-art dense-to-sparse method, GMP. We also test whether a small dense network and a static sparse network with the same number of parameters as Selfish-RNN can match the performance of Selfish-RNN. We train a dense stacked LSTMs with 700 hidden units, named as "Small Dense". In line with the previous studies (Mocanu et al., 2018; Mostafa & Wang, 2019; Evci et al., 2020), both static sparse networks and small dense networks fall short of Selfish-RNN. Moreover, training a static sparse network from scratch with uniform distribution performs better than the one with *ER* distribution.

To understand better the effect of different optimizers on different DST methods, we report the performance of all DST methods trained with Adam, momentum SGD, and SNT-ASGD. For SNFS (SNT-ASGD), we replace momentum of weights with their gradients, as SNT-ASGD does not

Table 3. Effect of different optimizers on different DST methods. We choose stacked LSTMs on PTB dataset at a sparsity level of 67%.

MODELS	#PARAMETERS	VALIDATION	TEST
DENSE	66.0M	82.57	78.57
		ADAM	
DSR	21.8M	89.95	88.16
SNFS	21.8M	88.31	86.28
RIGL	21.8M	88.39	85.61
SET	21.8M	87.30	85.49
SELFISH-RNN	21.8M	**85.70**	**82.85**
		SGD WITH MOMENTUM	
SNFS	21.8M	90.09	87.98
SET	21.8M	85.73	82.52
RIGL	21.8M	84.78	80.81
DSR	21.8M	82.89	80.09
SELFISH-RNN	21.8M	**82.48**	**79.69**
		SNT-ASGD	
SNFS	21.8M	82.11	79.50
RIGL	21.8M	78.31	75.90
SET	21.8M	76.78	74.84
SELFISH-RNN	21.8M	73.76	71.65
DSR	21.8M	**72.30**	**70.76**

involve any momentum terms. We use the same hyperparameters for all DST methods. The results are shown in Table 3. It is clear that SNT-ASGD brings significant perplexity improvements to all sparse training techniques. This further stands as empirical evidence that SNT-ASGD is crucial to improve the sparse training performance in the RNN setting. Moreover, compared with other DST methods, Selfish-RNN is quite robust to the choice of optimizers likely due to its simple scheme to update the sparse connectivity. Advanced strategies such as across-layer weight redistribution used in DSR and SNFS, gradient-based weight growth used in RigL and SNFS heavily depend on optimizers. They might work decently for some optimization methods but may not for others.

4.2. Recurrent Highway Networks

Recurrent Highway Networks (Zilly et al., 2017) is a variant of RNNs allowing RNNs to explore deeper architectures inside the recurrent transition. The results are shown in the right side of Table 2. Again, Selfish-RNN achieves the lowest perplexity with both Adam and SNT-ASGD, better than the dense-to-sparse methods (ISS and GMP). Surprisingly, random-based growth methods (SET, DSR, and Selfish-RNN) consistently have the lower perplexity than the gradient-based growth methods (RigL and SNFS). We further analyze the effect of different weight growth methods on DST in Section 5.2.

5. Analyzing the Performance of Selfish-RNN

5.1. Analysis of Topological Distance between Sparse Connectivities

Prior works on understanding dense loss landscapes have shown the existence of diverse low-loss solutions on the manifold of dense networks (Goodfellow et al., 2014; Garipov et al., 2018; Draxler et al., 2018; Fort & Jastrzebski, 2019). Here, the fact that Selfish-RNN consistently achieves good performance with different runs naturally raises some questions: e.g., are final sparse connectivities obtained by different runs similar or very different? Is the distance between the original sparse connectivity and the final sparse connectivity large or small? To answer these questions, we investigate a method based on graph edit distance (GED) (Sanfeliu & Fu, 1983) to measure the topological distance between different sparse connectivities. The distance is scaled between 0 and 1. The smaller the distance is, the more similar the two sparse topologies are (See Appendix J for details on how we measure the sparse connectivity distance).

The results are demonstrated in Figure 4. Figure 4-left shows how the topology of one random-initialized (random sparse connectivity and random weight values) network evolves when trained with Selfish-RNN. We compare the sparse connectivity at 5 epoch with those at the following epochs. We can see that the distance gradually increases from 0 to a very high value 0.8, meaning that Selfish-RNN optimizes the initial topology to a very different one. Moreover, Figure 4-right illustrates that the topological distance between two same-initialized (same sparse connectivity and same weight values) networks trained with different seeds after the 4^{th} epoch. Started from the same sparse topology, they evolve to completely different sparse topologies. While topologically different, they have very similarly performance. This indicates that in the case of RNNs there exist many low-dimensional sub-networks that can achieve similarly low loss. This phenomenon complements the findings of Liu et al. (2020c) which shows that there are numerous sparse sub-networks performing similarly well in the context of sparse MLPs.

5.2. Analysis of Weight Growth Methods

Methods that leverage gradient-based weight growth (SNFS and RigL) have shown superiority on performance over the methods using random-based weight growth for CNNs (Evci et al., 2020). However, we observe a different behavior with RNNs. We set up a controlled experiment to compare these two methods with SNT-ASGD and momentum SGD. We report the results with various update intervals (the number of iterations between sparse connectivity updates) in Figure 5. Surprisingly, gradient-based growth performs worse than random-based growth in most cases. Our hypothesis

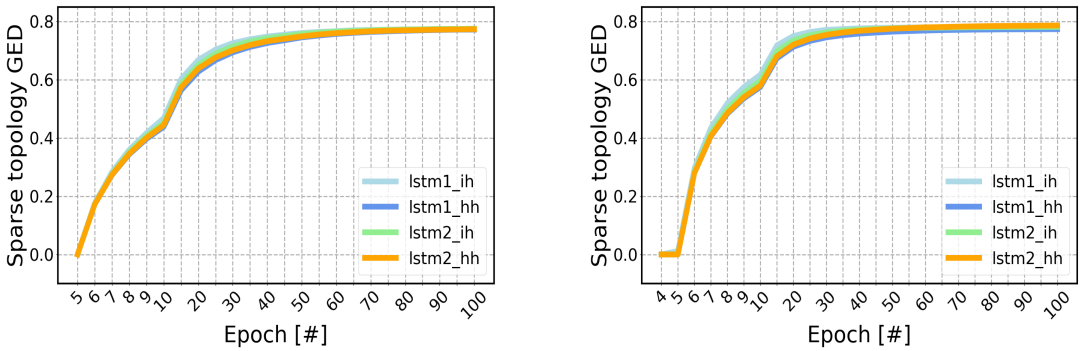


Figure 4. (**left**) One random-initialized sparse stacked LSTMs trained with Selfish-RNN end up with a very different sparse connectivity topology. (**right**) Two same-initialized sparse stacked LSTMs trained with different random seeds end up with very different sparse connectivity topologies. ih is the input weight tensor comprising four cell gates and hh is the hidden state weight tensor comprising four cell gates.

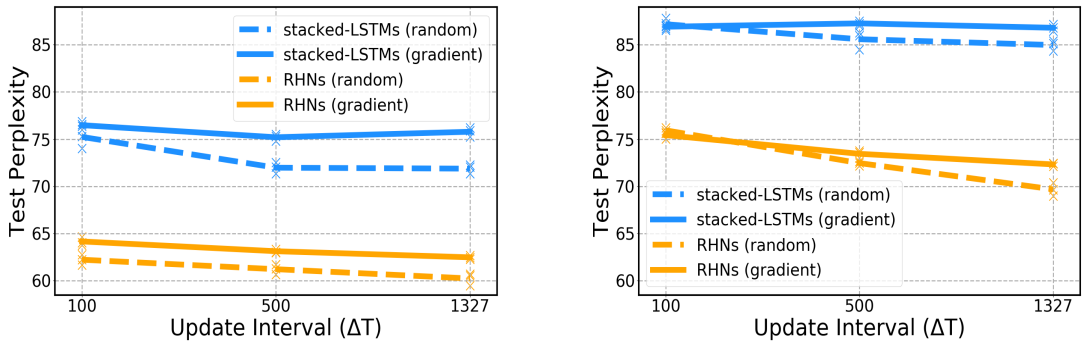


Figure 5. Comparison between random-based growth and gradient-based growth. (**left**) Models trained with SNT-ASGD. (**right**) Models trained with momentum SGD.

is that random growth helps in exploring better the search space, as it naturally considers a large number of various sparse connectivities during training, which is crucial to the performance of dynamic sparse training. Differently, gradient growth drives the network topology towards some similar local optima for the sparse connectivity as it uses a greedy search strategy (highest gradient magnitude) at every topological change. However, benefits provided by high-magnitude gradients might change dynamically afterwards due to complicated interactions between weights. We empirically illustrate our hypothesis via the proposed sparse connectivity distance measurement in Appendix K.

5.3. Analysis of Sparse Initialization

It has been shown that the choice of sparse initialization (sparsity distribution) is important for sparse training in Frankle & Carbin (2019); Kusupati et al. (2020); Evci et al. (2020). Here, we compare two types of sparse initialization for RNNs, ER distribution and uniform distribution. Uniform distribution namely enforces the sparsity level of each layer to be the same as S. ER distribution allocates higher sparsity to larger layers than smaller ones. Note that its variant *Erdős-Rényi-Kernel* proposed by Evci et al. (2020) scales back to ER for RNNs, as no kernels are involved. The results are shown as the *Static* group in Table 2. We can see that uniform distribution outperforms ER distribution consistently for RNNs.

5.4. Analysis of DST Hyperparameters

The sparsity S and the initial pruning rate p are two hyperparameters of our DST method. We show their sensitivity analysis in Appendix F and Appendix G. We find that Selfish Stacked LSTMs, RHNs, ON-LSTM, and AWD-LSTM-MoS need around 25%, 40%, 45%, and 40% parameters to reach the performance of their dense counterparts, respectively. In addition, our method is quite robust to the choice of the initial pruning rate.

6. Conclusion

In this paper, we developed an approach to train sparse RNNs from scratch with a fixed parameter count throughout training. We further proposed SNT-ASGD, a specially designed sparse optimizer for training sparse RNNs and showed that it substantially improves the performance of all DST methods in RNNs. We observed that random-based growth achieves lower perplexity than gradient-based growth in the case of RNNs. Further, we developed an approach to compare two different sparse connectivities from the perspective of graph theory. Using this approach, we found that random-based growth explores better the topological search space for optimal sparse connectivities, whereas gradient-based growth is prone to drive the network towards similar sparse connectivity patterns, opening the path for a better understanding of sparse training.

References

Bellec, G., Kappel, D., Maass, W., and Legenstein, R. Deep rewiring: Training very sparse deep networks. In *International Conference on Learning Representations*, 2018. URL https://openreview.net/forum?id=BJ_wN01C-.

Dai, R., Li, L., and Yu, W. Fast training and model compression of gated rnns via singular value decomposition. In *2018 International Joint Conference on Neural Networks (IJCNN)*, pp. 1–7. IEEE, 2018.

de Jorge, P., Sanyal, A., Behl, H. S., Torr, P. H., Rogez, G., and Dokania, P. K. Progressive skeletonization: Trimming more fat from a network at initialization. *arXiv preprint arXiv:2006.09081*, 2020.

Dettmers, T. and Zettlemoyer, L. Sparse networks from scratch: Faster training without losing performance. *arXiv preprint arXiv:1907.04840*, 2019.

Draxler, F., Veschgini, K., Salmhofer, M., and Hamprecht, F. A. Essentially no barriers in neural network energy landscape. *arXiv preprint arXiv:1803.00885*, 2018.

Elman, J. L. Finding structure in time. *Cognitive science*, 14(2):179–211, 1990.

Evci, U., Gale, T., Menick, J., Castro, P. S., and Elsen, E. Rigging the lottery: Making all tickets winners. In *International Conference on Machine Learning*, 2020.

Fort, S. and Jastrzebski, S. Large scale structure of neural network loss landscapes. In *Advances in Neural Information Processing Systems*, pp. 6709–6717, 2019.

Frankle, J. and Carbin, M. The lottery ticket hypothesis: Finding sparse, trainable neural networks. In *International Conference on Learning Representations*, 2019. URL https://openreview.net/forum?id=rJl-b3RcF7.

Gal, Y. and Ghahramani, Z. A theoretically grounded application of dropout in recurrent neural networks. In *Advances in neural information processing systems*, pp. 1019–1027, 2016.

Gale, T., Elsen, E., and Hooker, S. The state of sparsity in deep neural networks. *arXiv preprint arXiv:1902.09574*, 2019.

Garipov, T., Izmailov, P., Podoprikhin, D., Vetrov, D. P., and Wilson, A. G. Loss surfaces, mode connectivity, and fast ensembling of dnns. In *Advances in Neural Information Processing Systems*, pp. 8789–8798, 2018.

Goodfellow, I. J., Vinyals, O., and Saxe, A. M. Qualitatively characterizing neural network optimization problems. *arXiv preprint arXiv:1412.6544*, 2014.

Grave, E., Joulin, A., and Usunier, N. Improving neural language models with a continuous cache. In *International Conference on Learning Representations*, 2017. URL https://openreview.net/forum?id=B184E5qee.

Gray, S., Radford, A., and Kingma, D. P. Gpu kernels for block-sparse weights. *arXiv preprint arXiv:1711.09224*, 3, 2017.

Han, S., Pool, J., Tran, J., and Dally, W. Learning both weights and connections for efficient neural network. In *Advances in neural information processing systems*, pp. 1135–1143, 2015.

Han, S., Mao, H., and Dally, W. J. Deep compression: Compressing deep neural networks with pruning, trained quantization and huffman coding. In *International Conference on Learning Representations*, 2016.

Hinton, G., Vinyals, O., and Dean, J. Distilling the knowledge in a neural network. *arXiv preprint arXiv:1503.02531*, 2015.

Hirschman, L., Light, M., Breck, E., and Burger, J. D. Deep read: A reading comprehension system. In *Proceedings of the 37th annual meeting of the Association for Computational Linguistics*, pp. 325–332, 1999.

Hochreiter, S. and Schmidhuber, J. Long short-term memory. *Neural computation*, 9(8):1735–1780, 1997.

Inan, H., Khosravi, K., and Socher, R. Tying word vectors and word classifiers: A loss framework for language modeling. In *International Conference on Learning Representations*, 2017.

Jaderberg, M., Vedaldi, A., and Zisserman, A. Speeding up convolutional neural networks with low rank expansions. *arXiv preprint arXiv:1405.3866*, 2014.

Janowsky, S. A. Pruning versus clipping in neural networks. *Physical Review A*, 39(12):6600, 1989.

Jayakumar, S., Pascanu, R., Rae, J., Osindero, S., and Elsen, E. Top-kast: Top-k always sparse training. *Advances in Neural Information Processing Systems*, 33, 2020.

Kalchbrenner, N. and Blunsom, P. Recurrent continuous translation models. In *Proceedings of the 2013 Conference on Empirical Methods in Natural Language Processing*, pp. 1700–1709, 2013.

Kalchbrenner, N., Elsen, E., Simonyan, K., Noury, S., Casagrande, N., Lockhart, E., Stimberg, F., Oord, A. v. d., Dieleman, S., and Kavukcuoglu, K. Efficient neural audio synthesis. In *International Conference on Learning Representations*, 2018.

Kepner, J. and Robinett, R. Radix-net: Structured sparse matrices for deep neural networks. In *2019 IEEE International Parallel and Distributed Processing Symposium Workshops (IPDPSW)*, pp. 268–274. IEEE, 2019.

Kingma, D. P. and Ba, J. Adam: A method for stochastic optimization. *arXiv preprint arXiv:1412.6980*, 2014.

Kingma, D. P., Salimans, T., and Welling, M. Variational dropout and the local reparameterization trick. *arXiv preprint arXiv:1506.02557*, 2015.

Krause, B., Kahembwe, E., Murray, I., and Renals, S. Dynamic evaluation of neural sequence models. In *International Conference on Machine Learning*, pp. 2766–2775, 2018.

Kusupati, A., Ramanujan, V., Somani, R., Wortsman, M., Jain, P., Kakade, S., and Farhadi, A. Soft threshold weight reparameterization for learnable sparsity. In *International Conference on Machine Learning*, pp. 5544–5555. PMLR, 2020.

LeCun, Y., Denker, J. S., and Solla, S. A. Optimal brain damage. In *Advances in neural information processing systems*, pp. 598–605, 1990.

Lee, N., Ajanthan, T., and Torr, P. SNIP: SINGLE-SHOT NETWORK PRUNING BASED ON CONNECTION SENSITIVITY. In *International Conference on Learning Representations*, 2019. URL https://openreview.net/forum?id=B1VZqjAcYX.

Lee, N., Ajanthan, T., Gould, S., and Torr, P. H. S. A signal propagation perspective for pruning neural networks at initialization. In *International Conference on Learning Representations*, 2020. URL https://openreview.net/forum?id=HJeTo2VFwH.

Li, Y., Yosinski, J., Clune, J., Lipson, H., and Hopcroft, J. E. Convergent learning: Do different neural networks learn the same representations? In *Iclr*, 2016.

Liu, J., XU, Z., SHI, R., Cheung, R. C. C., and So, H. K. Dynamic sparse training: Find efficient sparse network from scratch with trainable masked layers. In *International Conference on Learning Representations*, 2020a. URL https://openreview.net/forum?id=SJlbGJrtDB.

Liu, S., Mocanu, D. C., and Pechenizkiy, M. Intrinsically sparse long short-term memory networks. *arXiv preprint arXiv:1901.09208*, 2019.

Liu, S., Mocanu, D. C., Matavalam, A. R. R., Pei, Y., and Pechenizkiy, M. Sparse evolutionary deep learning with over one million artificial neurons on commodity hardware. *Neural Computing and Applications*, pp. 1–16, 2020b.

Liu, S., van der Lee, T., Yaman, A., Atashgahi, Z., Ferrar, D., Sokar, G., Pechenizkiy, M., and Mocanu, D. Topological insights into sparse neural networks. In *Joint European Conference on Machine Learning and Knowledge Discovery in Databases*, 2020c.

Louizos, C., Welling, M., and Kingma, D. P. Learning sparse neural networks through l_0 regularization. In *International Conference on Learning Representations*, 2017.

Ma, R., Miao, J., Niu, L., and Zhang, P. Transformed l1 regularization for learning sparse deep neural networks. *Neural Networks*, 119:286–298, 2019.

Marcus, M., Santorini, B., and Marcinkiewicz, M. A. Building a large annotated corpus of english: The penn treebank. 1993.

Melis, G., Dyer, C., and Blunsom, P. On the state of the art of evaluation in neural language models. *arXiv preprint arXiv:1707.05589*, 2017.

Melis, G., Dyer, C., and Blunsom, P. On the state of the art of evaluation in neural language models. In *International Conference on Learning Representations*, 2018. URL https://openreview.net/forum?id=ByJHuTgA-.

Merity, S., Xiong, C., Bradbury, J., and Socher, R. Pointer sentinel mixture models. In *International Conference on Learning Representations*, 2017.

Merity, S., Keskar, N. S., and Socher, R. Regularizing and optimizing LSTM language models. In *International Conference on Learning Representations*, 2018. URL https://openreview.net/forum?id=SyyGPP0TZ.

Mikolov, T., Karafiát, M., Burget, L., Černockỳ, J., and Khudanpur, S. Recurrent neural network based language model. In *Eleventh annual conference of the international speech communication association*, 2010.

Mocanu, D. C., Mocanu, E., Nguyen, P. H., Gibescu, M., and Liotta, A. A topological insight into restricted boltzmann machines. *Machine Learning*, 104(2):243–270, Sep 2016. ISSN 1573-0565. doi: 10.1007/s10994-016-5570-z. URL https://doi.org/10.1007/s10994-016-5570-z.

Mocanu, D. C., Mocanu, E., Stone, P., Nguyen, P. H., Gibescu, M., and Liotta, A. Scalable training of artificial neural networks with adaptive sparse connectivity inspired by network science. *Nature Communications*, 9 (1):2383, 2018.

Molchanov, D., Ashukha, A., and Vetrov, D. Variational dropout sparsifies deep neural networks. In *Proceedings of the 34th International Conference on Machine Learning-Volume 70*, pp. 2498–2507. JMLR. org, 2017.

Molchanov, P., Tyree, S., Karras, T., Aila, T., and Kautz, J. Pruning convolutional neural networks for resource efficient inference. *arXiv preprint arXiv:1611.06440*, 2016.

Moradi, R., Berangi, R., and Minaei, B. Sparsemaps: convolutional networks with sparse feature maps for tiny image classification. *Expert Systems with Applications*, 119: 142–154, 2019.

Mostafa, H. and Wang, X. Parameter efficient training of deep convolutional neural networks by dynamic sparse reparameterization. In *International Conference on Machine Learning*, 2019.

Mozer, M. C. and Smolensky, P. Using relevance to reduce network size automatically. *Connection Science*, 1(1): 3–16, 1989.

NVIDIA. Nvidia a100 tensor core gpu architecture. *Retrieved from: https://www.nvidia.com/content/dam/en-zz/Solutions/Data-Center/nvidia-ampere-architecture-whitepaper.pdf*, 2020.

Polyak, B. T. and Juditsky, A. B. Acceleration of stochastic approximation by averaging. *SIAM Journal on Control and Optimization*, 30(4):838–855, 1992.

Prabhu, A., Varma, G., and Namboodiri, A. Deep expander networks: Efficient deep networks from graph theory. In *Proceedings of the European Conference on Computer Vision (ECCV)*, pp. 20–35, 2018.

Raihan, M. A. and Aamodt, T. M. Sparse weight activation training. *arXiv preprint arXiv:2001.01969*, 2020.

Sanfeliu, A. and Fu, K.-S. A distance measure between attributed relational graphs for pattern recognition. *IEEE transactions on systems, man, and cybernetics*, (3):353–362, 1983.

Saxe, A. M., McClelland, J. L., and Ganguli, S. Exact solutions to the nonlinear dynamics of learning in deep linear neural networks. *ICLR*, 2014.

Shen, Y., Tan, S., Sordoni, A., and Courville, A. Ordered neurons: Integrating tree structures into recurrent neural networks. In *International Conference on Learning Representations*, 2019. URL https://openreview.net/forum?id=B1l6qiR5F7.

Srivastava, R. K., Greff, K., and Schmidhuber, J. Training very deep networks. In *Advances in neural information processing systems*, pp. 2377–2385, 2015.

Tanaka, H., Kunin, D., Yamins, D. L., and Ganguli, S. Pruning neural networks without any data by iteratively conserving synaptic flow. *arXiv preprint arXiv:2006.05467*, 2020.

Wang, C., Zhang, G., and Grosse, R. Picking winning tickets before training by preserving gradient flow. In *International Conference on Learning Representations*, 2020. URL https://openreview.net/forum?id=SkgsACVKPH.

Wang, S. and Jiang, J. Machine comprehension using match-lstm and answer pointer. In *International Conference on Learning Representations*, 2017.

Wen, W., He, Y., Rajbhandari, S., Zhang, M., Wang, W., Liu, F., Hu, B., Chen, Y., and Li, H. Learning intrinsic sparse structures within long short-term memory. In *International Conference on Learning Representations*, 2018. URL https://openreview.net/forum?id=rk6cfpRjZ.

Xiao, X., Wang, Z., and Rajasekaran, S. Autoprune: Automatic network pruning by regularizing auxiliary parameters. *Advances in neural information processing systems*, 32, 2019.

Yang, J. and Ma, J. Feed-forward neural network training using sparse representation. *Expert Systems with Applications*, 116:255–264, 2019.

Yang, Z., Dai, Z., Salakhutdinov, R., and Cohen, W. W. Breaking the softmax bottleneck: A high-rank RNN language model. In *International Conference on Learning Representations*, 2018. URL https://openreview.net/forum?id=HkwZSG-CZ.

Zaremba, W., Sutskever, I., and Vinyals, O. Recurrent neural network regularization. *arXiv preprint arXiv:1409.2329*, 2014.

Zhou, H., Lan, J., Liu, R., and Yosinski, J. Deconstructing lottery tickets: Zeros, signs, and the supermask. In *Advances in Neural Information Processing Systems*, pp. 3597–3607, 2019.

Zhu, M. and Gupta, S. To prune, or not to prune: exploring the efficacy of pruning for model compression. *arXiv preprint arXiv:1710.01878*, 2017.

Zilly, J. G., Srivastava, R. K., Koutník, J., and Schmidhuber, J. Recurrent highway networks. In *Proceedings of the 34th International Conference on Machine Learning-Volume 70*, pp. 4189–4198. JMLR. org, 2017.

Appendices

A. Hyperparameters

In this section, we share the hyperparameters used in thie paper. For fair comparison, we use the exact same hyperparameters and regularization introduced in ON-LSTM (Shen et al., 2019) and AWD-LSTM-MoS (Yang et al., 2018). We then extend the similar settings to stacked LSTMs and RHNs. No hyperparameter tuning techniques such as Melis et al. (2017) are involved in our experiments. No need of finetuning the original hyperparameters of the dense model is another advantage of our method. For all DST methods, the hyperparameters are the same, as shared in Table 4.

B. Ablation Study

To analyze the influence of cell gate redistribution and Sparse NT-ASGD on the performance of sparse RNN training, we conduct an ablation study for all architectures. All models use the same hyperparameters with the ones reported in the main paper. We present the validation and testing perplexity for variants of our model without these two contributions, as shown in Table 5. Not surprisingly, removing either of these two novelties degrades the performance. There is a significant degradation in the performance for all models, up to 13 perplexity point, if the optimizer switches to the standard NT-ASGD. This stands as empirical evidence regarding the benefit of SNT-ASGD. Without cell gate redistribution, the testing perplexity of all models degrades except for RHNs whose number of redistributed weights in each layer is only two. This indicates that cell gate redistribution is more effective for the models with more cell gates.

C. Comparison of Different Cell Gate Redistribution Methods

In Table 6, we conduct a small experiment to compare different methods of cell gate redistribution with stacked LSTMs. We consider weight redistribution based on the mean value of the magnitude of nonzero weights and the mean value of the gradient magnitude of nonzero weights. Our method can achieve the lowest perplexity.

D. Experimental Results with ON-LSTM

Proposed by Shen et al. (2019) recently, ON-LSTM can learn the latent tree structure of natural language by learning the order of neurons. For a fair comparison, we use exactly the same model hyper-parameters and regularization used in ON-LSTM. We set the sparsity of each layer to 55% and the initial pruning rate to 0.5. Same as ON-LSTM, we train the model for 1000 epochs and restart SNT-ASGD as a fine-tuning step once at the 500^{th} epoch, dubbed as Selfish-RNN$_{1000}$. As shown in Table 7, Selfish-RNN outperforms the dense model while reducing the model size to 11.3M. Without SNT-ASGD, sparse training techniques can not reduce the test perplexity to 60. SNT-ASGD is able to improve the performance of RigL by 5 perplexity. Moreover, one interesting observation is that one of the regularizations used in the standard ON-LSTM, DropConnect, is perfectly compatible with our method, although it also drops the hidden-to-hidden weights out randomly during training.

In our experiments we observe that Selfish-RNN benefits significantly from the second fine-tuning operation. We scale the learning schedule to 1300 epochs with two fine-tuning operations at epoch 500 and 1000, respectively, dubbed as Selfish-RNN$_{1300}$. It is interesting that Selfish-RNN$_{1300}$ can achieve lower testing perplexity after the second fine-tuning step, whereas the dense model Dense$_{1300}$ can not even reach again the perplexity that it had before the second fine-tuning. The heuristic explanation here is that our method helps the optimization escape the local optima or a local saddle point by optimizing the sparse structure, while for dense models whose energy landscape is fixed, it is very difficult for the optimizer to find its way off the saddle point or the local optima.

E. Experimental Results with AWD-LSTM-MoS

We also evaluate Selfish-RNN on the WikiText-2 dataset. The model we choose is AWD-LSTM-MoS (Yang et al., 2018), which is the state-of-the-art RNN-based language model. It replaces Softmax with *Mixture of Softmaxes* (MoS) to alleviate the Softmax bottleneck issue in modeling natural language. For a fair comparison, we exactly follow the model hyper-parameters and regularization used in AWD-LSTM-MoS. We sparsify all layers with 55% sparsity except for the prior layer as its number of parameters is negligible. We train our model for 1000 epochs without finetuning or dynamical evaluation (Krause et al., 2018) to simply show the effectiveness of our method. As demonstrated in Table 8, Selfish AWD-LSTM-MoS can match the performance of the corresponding dense model with 15.6M parameters.

F. Effect of Sparsity

There is a trade-off between the sparsity level S and the test perplexity of Selfish-RNN. When there are too few parameters, the sparse neural network will not have enough capacity to fit the data. Here, we analyze this trade-off by training all models with Selfish-RNN at various sparsity levels $S \in [0.50, 0.55, 0.60, 0.70, 0.80, 0.90]$, reported in Figure 6a. We find that Selfish Stacked LSTMs, RHNs,

Table 4. Experiment hyperparameters including Optimizer (Opt), Learning rate (Lr), Batch size (Bs), Backpropagation through time (BPTT), Clip norm (Clip), Non-monotone interval for SNT-ASGD (Nonmono), Initial pruning rate (P); Lr Drop with (A, B) refers to B epochs with no improvement after which learning rate will be reduced by a factor of A; Dropout refers to the word-level dropout, embedding dropout, hidden layer dropout, and output dropout, respectively; Coupled means that the carry gate and the transform gate are coupled in RHNs; Tied means reusing the input word embedding matrix as the output matrix.

Model	Data	Opt	Lr	Lr Drop	Bs	BPTT	Dropout	Epochs	Tied	Coupled	Clip	Nonmono	P
Stacked LSTMs	PTB	Adam SNT-ASGD Momentum SGD	0.001 40 2	(2x, 2) - (1.33x, 1)	20	35	(0, 0, 0.65, 0)	100	no	no	0.25	5	0.7
RHNs	PTB	Adam SNT-ASGD	0.001 15	(2x, 2) -	20	35	(0.2, 0.65, 0.25, 0.65)	500	yes	yes	0.25	5	0.5
ON-LSTM	PTB	Adam SNT-ASGD	0.001 30	(2x, 2) -	20	70	(0.1, 0.5, 0.3, 0.45)	1000	yes	no	0.25	5	0.5
AWD-LSTM-MoS	WikiText-2	Adam SNT-ASGD	0.001 15	(2x, 2) -	15	70	(0.1, 0.55, 0.2, 0.4)	1000	yes	no	0.25	5	0.5

Table 5. Ablation study of Selfish-RNN with stacked LSTMs, RHNs, ON-LSTM on Penn Treebank and AWD-LSTM-MoS on WikiText-2.

Methods	Stacked LSTMs	RHNs	ON-LSTM	AWD-LSTM-MoS
Selfish-RNN	71.65	60.35	55.68	63.05
w/o cell gate redistribution	72.89	60.26	57.48	65.27
w/o Sparse NT-ASGD	73.74	69.70	69.28	71.65

ON-LSTM, and AWD-LSTM-MoS need around 25%, 40%, 45%, and 40% parameters to reach the performance of their dense counterparts, respectively.

G. Effect of Initial pruning rate

The initial pruning rate p determines how many weights would be removed at each connectivity update. We analyze the performance sensitivity of our algorithm to the initial pruning rate p by varying it $\in [0.3, 0.5, 0.7]$. We set the sparsity level of each model as the one having the best performance in Figure 6a. Results are shown in Figure 6b. We can clearly see that our method is very robust to the choice of the initial pruning rate.

H. Difference Among SET, Selfish-RNN and Iterative Pruning Methods

The topology update strategy of Selfish-RNN differs from SET in several important features (1) we automatically redistribute weights across cell gates for better regularization, (2) we use magnitude-based removal instead of removing a fraction of the smallest positive weights and the largest negative weights, (3) we use uniform initialization rather than non-uniform sparse distribution like ER or ERK. Additionally, the optimizer proposed in this work, SNT-ASGD, brings substantial perplexity improvement to the sparse RNN training.

Iterative pruning and retraining techniques (Han et al., 2016; Zhu & Gupta, 2017; Frankle & Carbin, 2019) usually involve three steps (1) pre-training a dense model, (2) pruning the unimportant based on some criteria, and (3) re-training the pruned model to improve performance. The pruning and re-training cycle is required at least once, but may many times depending on the specific algorithms used. Therefore, the computational costs required by iterative pruning and retraining is at least the same as fully training a dense model. Different from iterative pruning and retraining, FLOPs required by Selfish-RNN is proportional to the density of the model, as it allows us to train a sparse network with a fixed number of parameters throughout training in one single run, without any retraining phases. Moreover, the overhead caused by the dynamic sparse connectivity operation is negligible, as it performs only once per epoch.

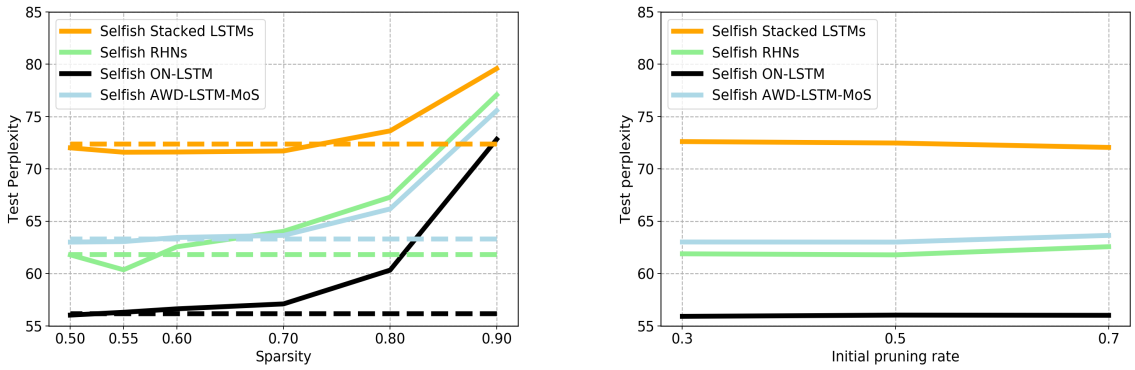
I. Comparison between Selfish-RNN and Pruning

It has been shown by Evci et al. (2020) that while state-of-the-art sparse training method (RigL) achieves promising performance with various CNN models, it fails to match the performance of pruning in RNNs. Given the fact that magnitude pruning has become a widely-used and strong baseline for model compression, we also report a comparison between Selfish-RNN and iterative magnitude pruning with stacked LSTMs. The pruning baseline is obtained from Zhu & Gupta (2017). The results are demonstrated in Figure 7-right.

We can see that Selfish-RNN exceeds the performance of pruning in most cases. An interesting phenomenon is that,

Table 6. A small experiment about the comparison among different cell gate redistribution methods. The experiment is evaluated with stacked LSTMs on Penn Treebank.

cell gate redistribution	#Param	Validation	Test
Mean of the magnitude of nonzero weights	21.8M	74.04	72.40
Mean of the gradient magnitude of nonzero weights	21.8M	74.54	72.31
Ours	21.8M	**73.76**	**71.65**



(a) Performance Sensitivity of Sparsity

(b) Performance Sensitivity of Pruning Rate

Figure 6. Sensitivity analysis of sparsity levels S and initial pruning rates p with Selfish stacked LSTMs, RHNs, ON-LSTM, and AWD-LSTM-MoS. (a) Test perplexity of all models with various sparsity levels. The initial pruning rate is 0.7 for stacked LSTMs, and 0.5 for the rest models. The dashed lines represent the performance of the corresponding dense models. (b) Test perplexity of all models with different initial pruning rates. The sparsity level is 67%, 52.8%, 55% and 55% for Selfish stacked LSTMs, RHNs, ON-LSTM, and AWD-LSTM-MoS, respectively.

Table 7. Single model perplexity on validation and test sets for the Penn Treebank language modeling task with ON-LSTM. Methods indicated with "ASGD" are trained with SNT-ASGD. The numbers reported are averaged over five runs.

Models	#Param	Val	Test
Dense_{1000} (NT-ASGD)	25M	58.29 ± 0.10	56.17 ± 0.12
Dense_{1300} (NT-ASGD)	25M	58.55 ± 0.11	56.28 ± 0.19
SET (Adam)	11.3M	65.90 ± 0.08	63.56 ± 0.14
DSR (Adam)	11.3M	65.22 ± 0.07	62.55 ± 0.06
SNFS (Adam)	11.3M	68.00 ± 0.10	65.52 ± 0.15
RigL (Adam)	11.3M	64.41 ± 0.05	62.01 ± 0.13
RigL_{1000} (ASGD)	11.3M	59.17 ± 0.08	57.23 ± 0.09
RigL_{1300} (ASGD)	11.3M	59.10 ± 0.05	57.44 ± 0.15
$\text{Selfish-RNN}_{1000}$ (ASGD)	11.3M	58.17 ± 0.06	56.31 ± 0.10
$\text{Selfish-RNN}_{1300}$ (ASGD)	11.3M	$\mathbf{57.67 \pm 0.03}$	$\mathbf{55.82 \pm 0.11}$

Table 8. Single model perplexity on validation and test sets for the WikiText-2 language modeling task with AWD-LSTM-MoS. Baseline is AWD-LSTM-MoS obtained from Yang et al. (2018). Methods with "ASGD" are trained with SNT-ASGD.

Models	#Param	Val	Test
Dense (NT-ASGD)	35M	66.01	63.33
SET (Adam)	15.6M	72.82	69.61
DSR (Adam)	15.6M	69.95	66.93
SNFS (Adam)	15.6M	79.97	76.18
RigL (Adam)	15.6M	71.36	68.52
RigL (ASGD)	15.6M	68.84	65.18
Selfish-RNN (ASGD)	15.6M	**65.96**	**63.05**

with increased sparsity, we see a decreased performance gap between Selfish-RNN and pruning. Especially, Selfish-RNN performs worse than pruning when the sparsity level is 95%. This can be attributed to the poor trainability problem of sparse models with extreme sparsity levels. Noted in Lee et al. (2020), the extreme sparse structure can break dynamical isometry (Saxe et al., 2014) of sparse networks, which subsequently degrades the trainability of sparse neural networks. Different from sparse training methods, pruning operates from a dense network and thus, does not have this problem.

J. Sparse Connectivity Distance Measurement

Our sparse connectivity distance measurement considers the unit alignment based on a *semi-matching* technique introduced by Li et al. (2016) and a graph distance measurement based on graph edit distance (GED) (Sanfeliu & Fu, 1983). More specifically, our measurement includes the following

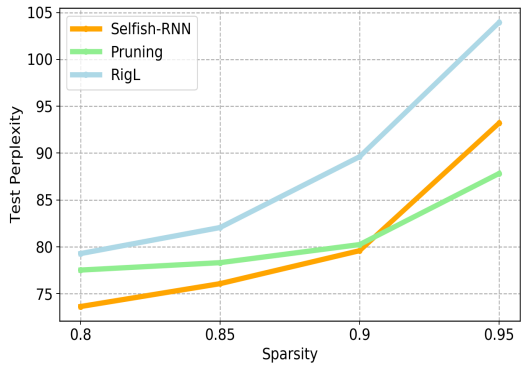


Figure 7. Comparison among Selfish-RNN, RigL and iterative magnitude pruning with stacked LSTMs on PTB. The pruning baseline is obtained from Zhu & Gupta (2017).

steps:

1. We train two sparse networks with dynamic sparse training on the training dataset and store the sparse topology after each epoch. Let $\boldsymbol{W}_l^i$ be the set of sparse topologies for the l-th layer of network i.

2. Using the saved model, we compute the activity output on the test data, $\boldsymbol{O}_l^i \in \mathbb{R}^{n \times m}$, where n is the number of hidden units and m is the number of samples.

3. We pair-wisely match two topologies obtained from different networks $\boldsymbol{W}_l^i$ and $\boldsymbol{W}_l^j$ by the semi-matching method introduced in Li et al. (2016) based on their activity units. The semi-matching step is achieved by finding the a pair of units from different networks with the maximum correlation.

4. After alignment, we apply graph edit distance (GED) to measure the similarity between $\boldsymbol{W}_l^i$ and $\boldsymbol{W}_l^j$. Eventually, the distance is scaled to lie between 0 and 1. The smaller the distance is, the more similar the two sparse topologies are.

Here, we choose stacked LSTMs on PTB dataset as a specific case to analyze. Specifically, we train two stacked LSTMs for 100 epochs with different random seeds. We choose a relatively small pruning rate of 0.1. We start alignment at the 5^{th} epoch to ensure a good alignment, as the model does not learn very well at the very beginning of training.

K. Sparse Connectivity Distance Comparison between Different Growth Methods

In this section, we investigate the topological distance between sparse connectivities learned by gradient weight growth and random weight growth. We empirically illustrate that gradient growth drives different networks into some similar connectivity patterns based on the proposed distance measurement between sparse connectivities. The initial pruning rates are set as 0.1 for all training runs in this section.

First, we measure the sparse connectivity distance between two different training runs trained with gradient growth and random growth, respectively, as shown in Figure 8. We can see that, starting with very different sparse connectivity topologies, two networks trained with random growth end up at the same distance, whereas the distance between two networks trained with gradient growth is continuously decreasing and this tendency is likely to continue as the training goes on. We further report the distance between two networks with same initialization (same sparse connectivity and same weight values) but different training seeds in Figure 9. We can see that the distance between sparse connectivities optimized by gradient growth is smaller than the ones optimized by random growth.

These observations are in line with our hypothesis and indicate that gradient growth drives networks into some similar structures, whereas random growth allows models to explore more sparse structures spanned over the dense network, and thus has a better chance to find a better sparse connectivity.

L. FLOPs Analysis of Different Approaches

Although different DST methods maintain a fix parameter count throughout training, their training costs can be very different since different sparse distributions lead to different computational costs. Hence, we also report the estimated training and inference FLOPs for all methods in this section.

We follow the way of calculating training FLOPs proposed by Evci et al. (2020). The perplexity and the corresponding training and inference FLOPs of different methods are given in Table 9. We split the process of training a sparse recurrent neural network into two steps: *forward pass* and *backward pass*.

Forward pass In order to calculate the loss of the current models given a batch of input data, the output of each layer is needed to be calculated based on a linear transformation and a non-linear activation function. Within each RNN layer, different cell gates are used to regulate information in sequence using the output of the previous time step and the input of this time step.

Backward pass In order to update weights, during the backward pass, each layer calculates 2 quantities: the gradient of the loss function with respect to the activations of the previous layer and the gradient of the loss function with

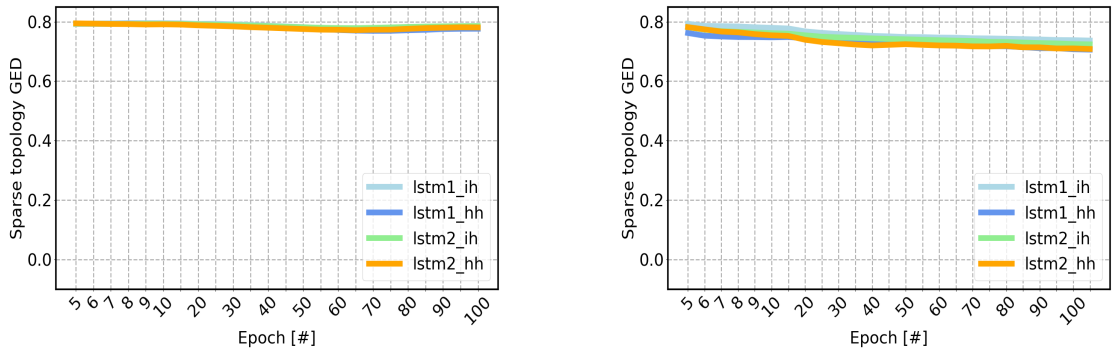


Figure 8. (**left**) The sparse connectivity distance between two different training runs of stacked LSTMs trained with random growth. (**right**) The sparse connectivity distance between two different training runs of stacked LSTMs trained with gradient growth.

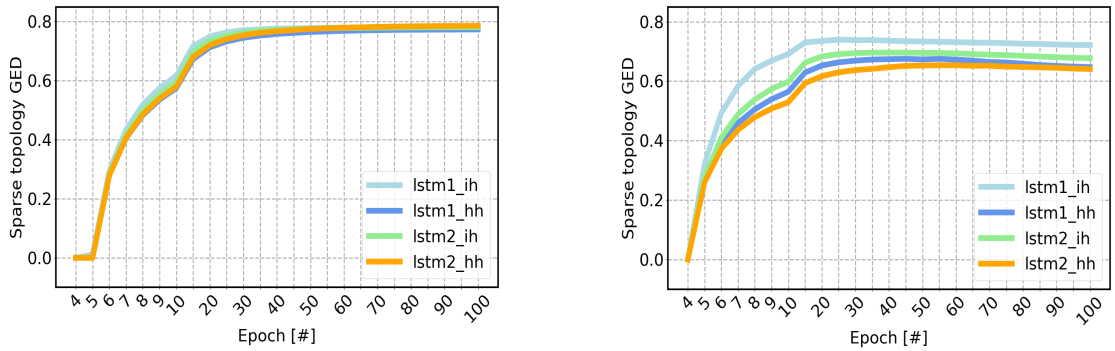


Figure 9. (**left**) The sparse connectivity distance between two stacked LSTMs with same initialization but different training seeds trained with random growth. (**right**) The sparse connectivity distance between two networks with same initialization but different training seeds trained with gradient growth. ih is the input weight tensor comprising four cell gates and hh is the hidden state weight tensor comprising four cell gates.

respect to its own weights. Therefore, the computational expense of *backward pass* is twice that of *forward pass*. Given that RNN models usually contain an embedding layer from which it is very efficient to pick a word vector, for models not using weight tying, we only count the computations to calculate the gradient of its parameters as the training FLOPs and we omit its inference FLOPs. For models using weight tying, both the training FLOPs and the inference FLOPs are omitted.

Given a specific architecture, we denote f_D as dense FLOPs required to finish one training iteration and f_S as the corresponding sparse FLOPs ($f_S \approx (1-S)f_D$), where S is the sparsity level. Thus $f_S \ll f_D$ for very sparse networks. Since different sparse training methods use different sparse distribution, their FLOPs f_S are also different from each other. We omit the FLOPs used to update the sparse connectivity, as it is only performed once per epoch. Overall, the total FLOPs required for one training update on one single sample are given in Table 10. The training FLOPs of dense-to-sparse methods like, ISS and pruning, are $3f_D * s_t$, where s_t is the sparsity of the model at iteration t. Since dense-to-sparse methods require to train a dense model for a while, their training FLOPs and memory requirement are higher than our method. For methods that allow the sparsity of each layer dynamically changing e.g., DSR and SNFS, we approximate their training FLOPs via their final distribution, as their sparse distribution converges to the final distribution in the first few epochs. ER distribution causes a bit more inference FLOPs than uniform distribution because it allocates more weights to the RNN layers than other layers. SNFS requires extra FLOPs to calculate dense momentum during the backward pass. Although RigL also uses the dense gradients to assist weight growth, it only needs to calculate dense gradients every ΔT iterations, thus with a smaller number of FLOPs given by $\frac{3f_S\Delta T+2f_S+f_D}{\Delta T+1}$. Here, we simply omit the extra FLOPs required by the full gradient calculation as it is negligible compared with the whole training FLOPs. Moreover, the inference FLOPs are calculated with the final sparse distribution learned by different methods.

Table 9. Single model perplexity on validation and test sets for the Penn Treebank language modeling task with stacked LSTMs and RHNs. FLOPs required to train the entire model and to test on single sample are reported. '*' indicates the reported results from the original papers: "Dense" is obtained from Zaremba et al. (2014) and ISS is obtained from Wen et al. (2018). "Static-ER" and "Static-uni" are the static sparse network trained from scratch with ER distribution and uniform distribution, respectively. "Small" refers the small-dense network.

	Stacked LSTMs				RHNs			
Models	FLOPs (Train)	FLOPs (Test)	Val	Test	FLOPs (Train)	FLOPs (Test)	Val	Test
Dense*	1x(3.1e16)	1x(7.2e10)	82.57	78.57	1x(6.5e16)	1x(3.3e10)	67.90	65.40
Dense (NT-ASGD)	1x	1x	74.51	72.40	1x	1x	63.44	61.84
	S=0.67				S=0.53			
Small (NT-ASGD)	0.33x	0.33x	88.67	86.33	0.47x	0.47x	70.10	68.40
Static-ER (SNT-ASGD)	0.33x	0.34x	81.02	79.30	0.47x	0.47x	75.74	73.21
Static-uni (SNT-ASGD)	0.33x	0.33x	80.37	78.61	0.47x	0.47x	74.11	71.83
ISS*	0.28x	0.20x	82.59	78.65	0.50x	0.47x	68.10	65.40
GMP (Adam)	0.63x	0.33x	89.47	87.97	0.62x	0.47x	63.21	61.55
SET (Adam)	0.33x	0.34x	87.30	85.49	0.47x	0.47x	63.66	61.08
DSR (Adam)	0.38x	0.40x	89.95	88.16	0.47x	0.47x	65.38	63.19
SNFS (Adam)	0.63x	0.38x	88.31	86.28	0.63x	0.45x	74.02	70.99
RigL (Adam)	0.33x	0.34x	88.39	85.61	0.47x	0.47x	67.43	64.41
Selfish-RNN (Adam)	0.33x	0.33x	85.70	82.85	0.47x	0.47x	63.28	60.75
GMP (SNT-ASGD)	0.63x	0.33x	76.78	74.84	0.62x	0.47x	65.63	63.96
RigL (SNT-ASGD)	0.33x	0.34x	78.31	75.90	0.47x	0.47x	64.82	62.47
Selfish-RNN (SNT-ASGD)	0.33x	0.33x	**73.76**	**71.65**	0.47x	0.47x	**62.10**	**60.35**
	S=0.62				S=0.68			
ISS*	0.32x	0.23x	80.24	76.03	0.34x	0.32x	70.30	67.70
GMP (SNT-ASGD)	0.63x	0.38x	74.86	73.03	0.51x	0.32x	66.61	64.98
RigL (SNT-ASGD)	0.38x	0.39x	77.16	74.76	0.32x	0.32x	69.32	66.64
Selfish-RNN (SNT-ASGD)	0.38x	0.38x	**73.50**	**71.42**	0.32x	0.32x	**66.35**	**64.03**

Table 10. Training FLOPs analysis of different sparse training approaches. f_D refers to the training FLOPs for a dense model to compute one single prediction in the *forward pass* and f_S refers to the training FLOPs for a sparse model. ΔT is the number of iterations used by RigL to update sparse connectivity. s_t is the sparsity level of the model at iteration t.

Method	Forward Pass	Backward Pass	Total
Dense	f_D	$2f_D$	$3f_D$
ISS	$f_D * s_t$	$2f_D * s_t$	$3f_D * s_t$
Pruning	$f_D * s_t$	$2f_D * s_t$	$3f_D * s_t$
SET	f_S	$2f_S$	$3f_S$
DSR	f_S	$2f_S$	$3f_S$
SNFS	f_S	$f_S + f_D$	$2f_S + f_D$
RigL	f_S	$\frac{(2\Delta T+1)f_S+f_D}{\Delta T+1}$	$\frac{3f_S\Delta T+2f_S+f_D}{\Delta T+1}$
Selfish-RNN (ours)	f_S	$2f_S$	$3f_S$

M. Final Cell Gate Sparsity Breakdown

We further investigate the final sparsity level of different cell gates learned automatically by our method in Figure 10. We find a consistent observation existing in all models, i.e., the weight of the forget gates, either the forget gate in the standard LSTM or the master forget gate in ON-LSTM, tend to be sparser than other gate weights. The weight of the cell gates and output gates are denser than the average. However, there is no big difference between the gates in RHNs, even

although the H nonlinear transform gate is slightly sparser than the T gate weight in most RHNs layers.

N. Limitation

The aforementioned training benefits have not been fully explored, as off-the-shelf software and hardware have limited support for sparse operations. The unstructured sparsity is difficult to be efficiently mapped to the existing parallel processors. The results of our paper provide motivation for new types of hardware accelerators and libraries with better support for sparse neural networks. Nevertheless, many recent works have been developed to accelerate sparse neural networks including Gray et al. (2017); Moradi et al. (2019); Ma et al. (2019); Yang & Ma (2019); Liu et al. (2020b). For instance, NVIDIA develops the A100 GPU enabling the Fine-Grained Structured Sparsity (NVIDIA, 2020). The sparse structure is enforced by allowing two nonzero values in every four-entry vector to reduce memory storage and bandwidth by almost $2\times$. We hope that our results will pile up on other researchers results in sparse training and soon there will be a change of perspective in such a way that the developers of deep learning software and hardware will start considering including real sparsity support in their solutions.

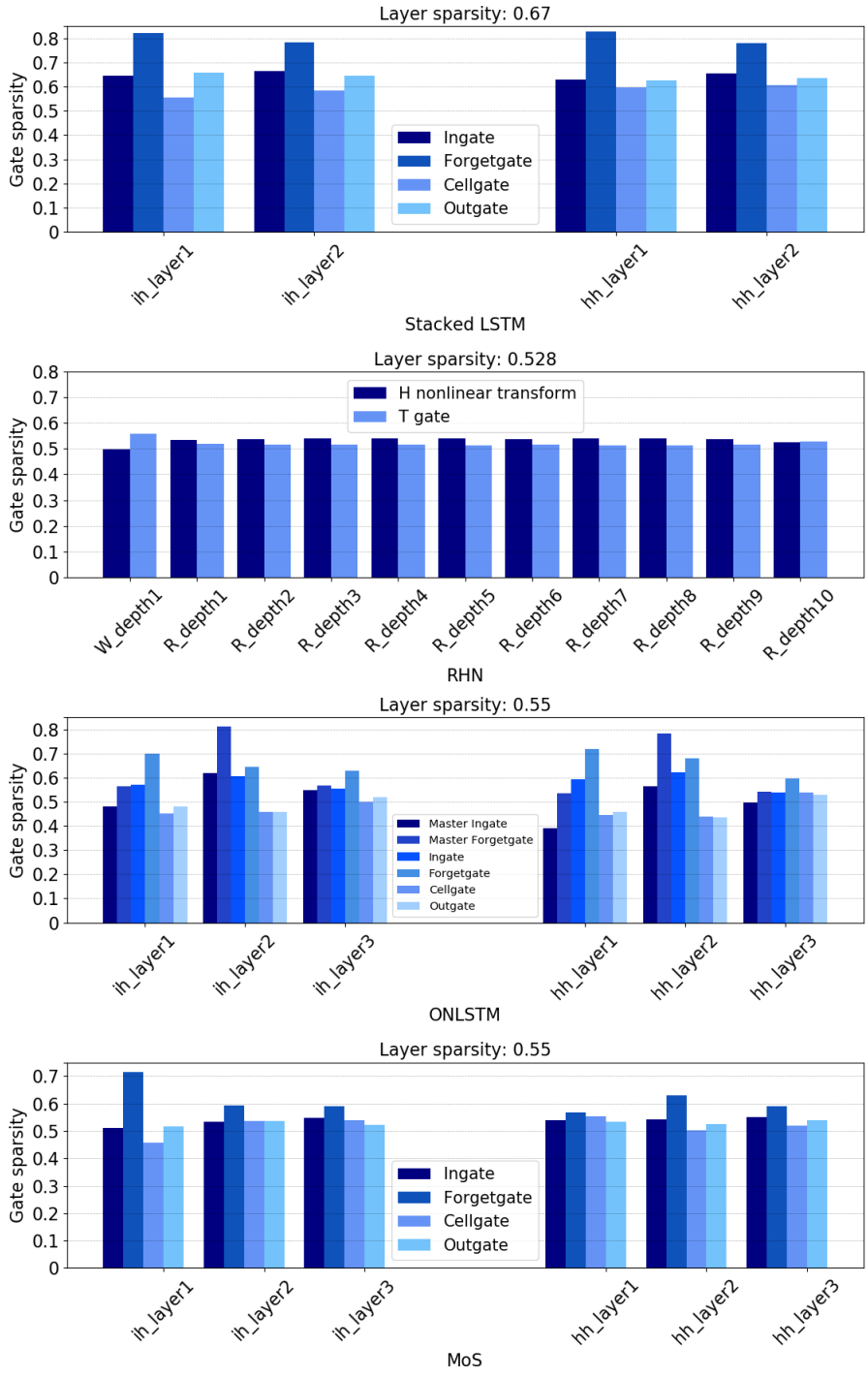


Figure 10. Breakdown of the final sparsity level of cell gates with stacked LSTMs, RHNs, ON-LSTM on PTB, AWD-LSTM-MoS on Wikitext-2. W and R is the weight of the H nonlinear transform and the T gate in RHNs, respectively; ih and hh refer to the input weight and the hidden weight of each LSTM layer, respectively.